Journal of Applied Polymer Science

Polyimide fibers prepared by a dry-spinning process: Enhanced mechanical properties of fibers containing biphenyl units

Shihua Wang, Jie Dong, Zhentao Li, Yuan Xu, Wenjun Tan, Xin Zhao, Qinghua Zhang
State Key Laboratory for the Modification of Chemical Fibers and Polymer Materials, College of Materials Science and Engineering, Donghua University, Shanghai 201620, People's Republic of China
Correspondence to: Q. Zhang (E-mail: qhzhang@dhu.edu.cn)

ABSTRACT: Polyimide (PI) fibers with enhanced mechanical properties and high thermal and dimensional stability were prepared via a two-step dry-spinning process through the introduction of 3,3′,4,4′-biphenyl tetracarboxylic dianhydride (BPDA) containing biphenyl units into rigid homopolyimide of pyromellitic dianhydride (PMDA) and 4,4′-oxydianiline. The attenuated total reflectance–Fourier transform infrared spectra results imply that the incorporated BPDA moieties accelerate the imidization process and increase the imidization degree (ID) of the precursor fibers; this was attributed to the increased molecular mobility of the polymer chains. Two-dimensional wide-angle X-ray diffraction spectra indicated that the prepared PI fibers possessed a well-defined crystal structure and polymer chains in the crystalline region were highly oriented along the fiber axis. The PI fiber, with the molar ratio of PMDA/BPDA being 7/3, showed optimum tensile strength and modulus values of 8.55 and 73.21 cN/dtex, respectively; these were attributed to the high IDs and molecular weights. Meanwhile, the PI fibers showed better dimensional stability than the commercial P84 fiber, and this is beneficial for its security applications. © 2016 Wiley Periodicals, Inc. J. Appl. Polym. Sci. **2016**, *133*, 43727.

KEYWORDS: fibers; mechanical properties; polyimides; structure-property relations; synthesis and processing

Received 10 December 2015; accepted 4 April 2016
DOI: 10.1002/app.43727

INTRODUCTION

Polymer fibers with excellent mechanical properties, thermal stability, and dimensional stability are of great interest for high-performance fiber-reinforced composites.[1–3] As important members in the family of high-tech polymeric fibers, aromatic polyimide (PI) fibers are attracting people's interests for their promising use in aerospace applications, membrane separation, and advanced composite because of their outstanding overall performances.[4–7]

Up to this point, real commercialized PI fibers have included P84 fibers (BTDA–TDI/MDI, where BTDA is 3,3′,4,4′-benzophenonetetracarboxylic dianhydride, TDI is toluene-2,4-diisocyanate and MDI is 4,4′-diphenylmethane diisocyanate) and Kermel fibers produced by Evonik Co., Ltd., and Kermel Co., Ltd., respectively. However, these two fibers are mainly fabricated by wet-spinning or dry-jet wet-spinning processes, and the diffusion process between the solvent and nonsolvent during the coagulation of precursor fibers can arouse microvoids in the fibers that reduce the mechanical properties of the fibers.[8–10] To solve this problem, recently, we reported a Kapton-type[11] PI fiber produced by the dry-spinning process.[12] The polymer was synthesized from pyromellitic dianhydride (PMDA) and 4,4′-oxydianiline (ODA) in dimethylacetamide (DMAc) with an intrinsic viscosity of 2.0 dL/g. First, a poly(amic acid) (PAA) solution was extruded into a heating column to get rid of the solvent to form a precursor fiber, and then, the precursor fiber was transformed to a PI fiber by heat treatment. Actually, another obvious advantage of the dry-spinning method depends on the fact that the as-spun fiber is relatively stable because of partial imidization at the heating column; this is conducive to solve the problem of the degradation of the as-spun fibers. In previous work, the imidization degree (ID) of the precursor fiber obtained under various spinning conditions was investigated with Fourier transform infrared (FTIR) spectroscopy and thermogravimetric analysis (TGA). The results show that the IDs of the as-spun fibers increased with elevating spinning temperature.[12] Because of the low molecular weights and rigid-rod structure of PMDA–ODA PAA, the mechanical properties of the prepared PI fiber were not so good.

To improve the mechanical properties of the dry-spun Kapton-type PI fiber, in this study, a series of copolyimide fibers with enhanced tensile strengths and moduli were developed via dry-spinning process based on a new design of introducing 3,3′,4,4′-biphenyl tetracarboxylic dianhydride (BPDA) containing biphenyl units into the rigid homopolyimide backbones of PMDA–ODA. The effects of the incorporated BPDA moieties on the ID, aggregation structure, and properties of the prepared fibers were investigated.

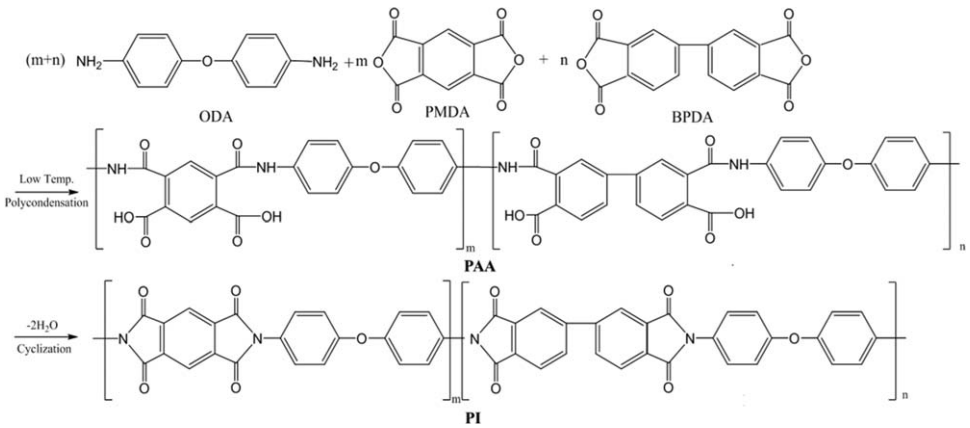

Scheme 1. Synthetic route for the copolyimide ($m/n = 10/0$, 9/1, 8/2, or 7/3). m and n, number of segments of PMDA-ODA and BPDA-ODA in the polymer chains, respectively.

EXPERIMENTAL

Materials

PMDA and BPDA were both purchased from Changzhou Sunlight Pharmaceutical Co., Ltd., and dried *in vacuo* at 120 °C for 24 h before use. ODA was obtained from Shandong Yantai Wanhua Co., Ltd. The solvent, DMAc, was provided by Jiangsu Aoshen New Materials Co., Ltd. Other commercially available reagent-grade chemicals were used without further purification.

Synthesis of the PMDA/ODA/BPDA PIs

Equimolar amounts of diamine and dianhydride monomers were used in all cases, and co-PAA solutions in DMAc were produced. Polymerization was carried out with various molar ratios of PMDA to BPDA:10/0 (PAA-0), 9/1 (PAA-1), 8/2 (PAA-2), and 7/3 (PAA-3). The reaction is shown in Scheme 1. A typical synthesis process was as follows: 600.7 g (3.0 mol) of ODA was added to 5.0 L of DMAc in a reaction container. Once the diamines were dissolved, 589.0 g (2.7 mol) of PMDA and 88.2 g (0.3 mol) of BPDA were gradually dropped into the previous solution with stirring for 2 h under dry nitrogen, and the PAA solution of PMDA/ODA/BPDA was thus prepared. The inherent viscosities of these PAA solutions were 2.16, 2.03, 2.45, and 2.88 dL/g, respectively. Apparently, the increase in the BPDA content resulted in an improvement in inherent viscosity ([η]) of the PAAs.

Preparation of the PI Fibers

Copolyimide solutions were filtered and degassed at 50 °C before spinning. The diagram of dry-spinning machine equipped with a 10 m vertical heating column is shown in Figure 1.[12] The precursor fibers were obtained by extruding PAA solution through the spinneret into the hot spinning column, solvent evaporation resulting in the solidified filaments. The as-spun PAA fibers were drawn through a heating tube with three temperature parts (400, 420, and 450 °C). The drawn ratios were controlled by the speeds by two taking up rollers. The prepared copolyimide fibers are also shown in Figure 1. In this work we prepared four PI fibers with various PMDA/BPDA molar ratios named PI-0 (10/0), PI-1(9/1), PI-2 (8/2), and PI-3 (7/3).

Characterization

The intrinsic viscosities of the PAA solutions were measured at 30 °C with an Ubbelohde viscometer with a capillary inner diameter of 0.5 mm. Attenuated total reflectance (ATR)–FTIR spectra of the prepared fibers were obtained at a resolution of 4 cm^{-1} on a Nicolet 8700 instrument with the range 4000–400 cm^{-1}. Single-fiber tensile testing was performed on a XQ 1-C instrument at an extension rate of 10 mm/min. Each sample was tested no fewer than 20 times to achieve an average value. TGA was conducted on a Netzsch 209 F3 at a heating rate of 5 °C/min. The dynamic mechanical properties [dynamic mechanical analysis (DMA)] and dimensional stability of the fibers were investigated by a DMA Q800 instrument in the range 30–550 °C under nitrogen. Two-dimensional wide-angle X-ray diffraction (WAXD) measurements were carried out at the Beamline Station (16B1) of the Shanghai Synchrotron Radiation Facility. The distance between the image plate (MAR CCD 165) and the samples was 150 mm, and the wavelength used was 0.124 nm. To obtain some sufficiently accurate information about the aggregation structure of the PI fibers, we used a

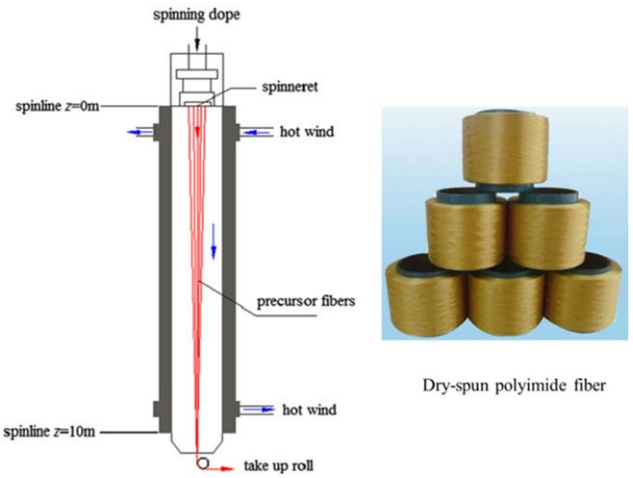

Figure 1. Flow process diagram for the preparation of PI fibers by a dry-spinning process and image of the dry-spun PI fibers. z, length of the hot spinning column. [Color figure can be viewed in the online issue, which is available at wileyonlinelibrary.com.]

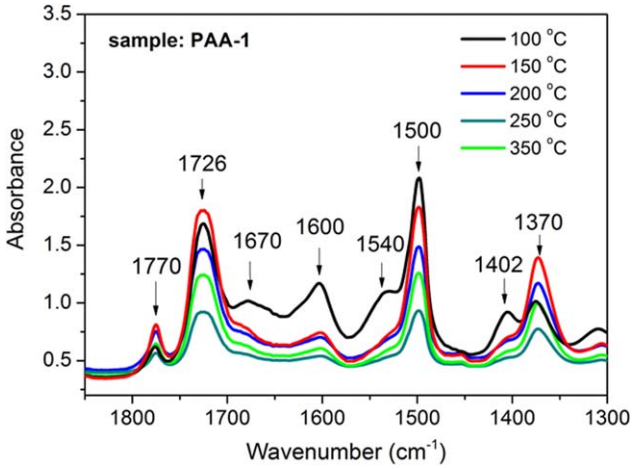

Figure 2. ATR–FTIR spectra of the PAA-1 precursor fibers as a function of the heating temperature. [Color figure can be viewed in the online issue, which is available at wileyonlinelibrary.com.]

typical image acquisition time of 50 s. The WAXD pattern was processed with the xPolar software package to correct for air scattering.

RESULTS AND DISCUSSION

Effects of BPDA on the ID of the Precursor PAA Fibers

The evolution of the chemical structure for the prepared PMDA/ODA/BPDA precursor fibers (PAA-1) in the imidization process was investigated with ATR–FTIR spectroscopy, as shown in Figure 2; the fibers went through dramatic changes during heat treatment from 100 to 350 °C. The imidization process of PAA-1 was easily identified by the disappearance of the amide-related bands and the appearance of the corresponding imide bands as the heating temperature increased. At 100 °C, the precursor PAA fiber vibrations included three bands: the carbonyl stretching of the carboxylic acid at 1726 cm^{-1}, the carbonyl stretching of the amide I mode at 1670 cm^{-1} (C═O, CONH), and the C—NH stretching of the amide II mode at 1540 cm^{-1}.[13] When it was heated to 300 °C, the characteristic peaks of the sample at 1370 and 1770 cm^{-1} were attributed to the C—N stretching and C═O symmetric stretching of the imide ring, respectively; these peaks illustrated the formation of fully imidized PI-1 fibers.[14,15]

In our last work,[16] we reported that the peak at 1370 cm^{-1} could be used to quantitatively calculate the ID by the following equation because of its very strong characteristic features:

$$\alpha = \frac{(D_{1370}/D_{1500})_{T1}}{(D_{1370}/D_{1500})_{T300}} \quad (1)$$

where α is the ID, and $(D_{1370}/D_{1500})_{T1}$ is the ratio of the height of the peak at 1370 cm^{-1} to that of the peak at 1500 cm^{-1} at the curing temperature (T_1), and $(D_{1370}/D_{1500})_{T300}$ is the ratio value after complete imidization at a curing temperature of 300 °C. The same method was used to evaluate the conversion degrees of the PAA-0, PAA-2, and PAA-3 precursor fibers. The IDs versus cyclization temperatures for these four samples are shown in Figure 3(A). These precursor dry-spun fibers showed various initial ID values, which ranged from 20 to 25% and depended on the molar ratios of BPDA; this was due to the partial imidization of the PAA fibers in the column. With an increase in the cyclization temperature to 180–200 °C, the IDs showed an abrupt increasing trend. When the temperature was continuously increased to 250 °C, the IDs changed slightly, and the values reached over 95%. This phenomenon is called the *kinetic stop of imidization* and was consistent with Christos' results.[17] Meanwhile, it is not difficult to determine that the ID of PAA-0 (PMDA/ODA) was lower than that of the other three samples containing BPDA units over the same reaction temperature, and the final degree of the PMDA/ODA/BPDA system was higher. Figure 3(B) shows the differential of the ID versus temperature. Obviously, PAA-3 exhibited the lowest peak temperature at 213.5 °C, whereas the corresponding peak temperature for PAA-0 increased to 229.8 °C; this indicated that the addition of BPDA into the polymer chains accelerated the imidization process. Kreuz *et al.*[18] explained that the change in the reactivity of the PAAs was a result of the diversification of the molecular mobility. In our case, the random copolymerization of PMDA/ODA/BPDA was beneficial for enhancing the mobility of the polymer chains. In the actual PI fabrication, the spinning temperature of PAA-0 was always 15 °C higher than that of the PAA-3 sample. This investigation developed a recommendable

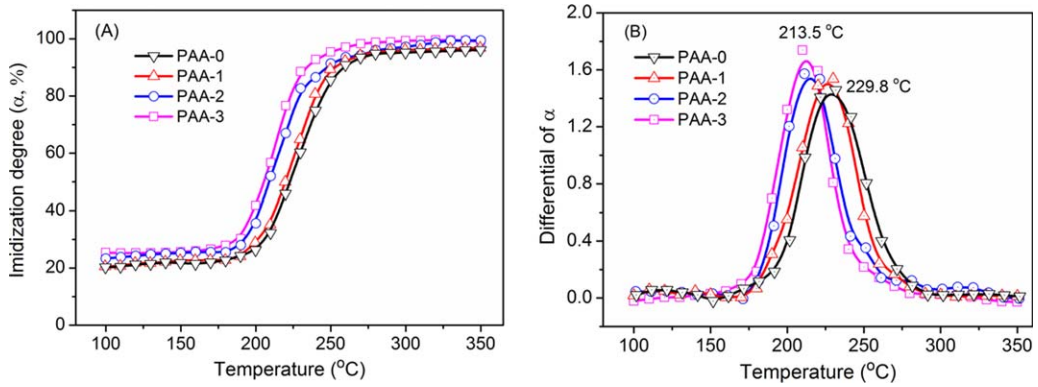

Figure 3. (A) ID versus temperature and (B) ID differential versus temperature. [Color figure can be viewed in the online issue, which is available at wileyonlinelibrary.com.]

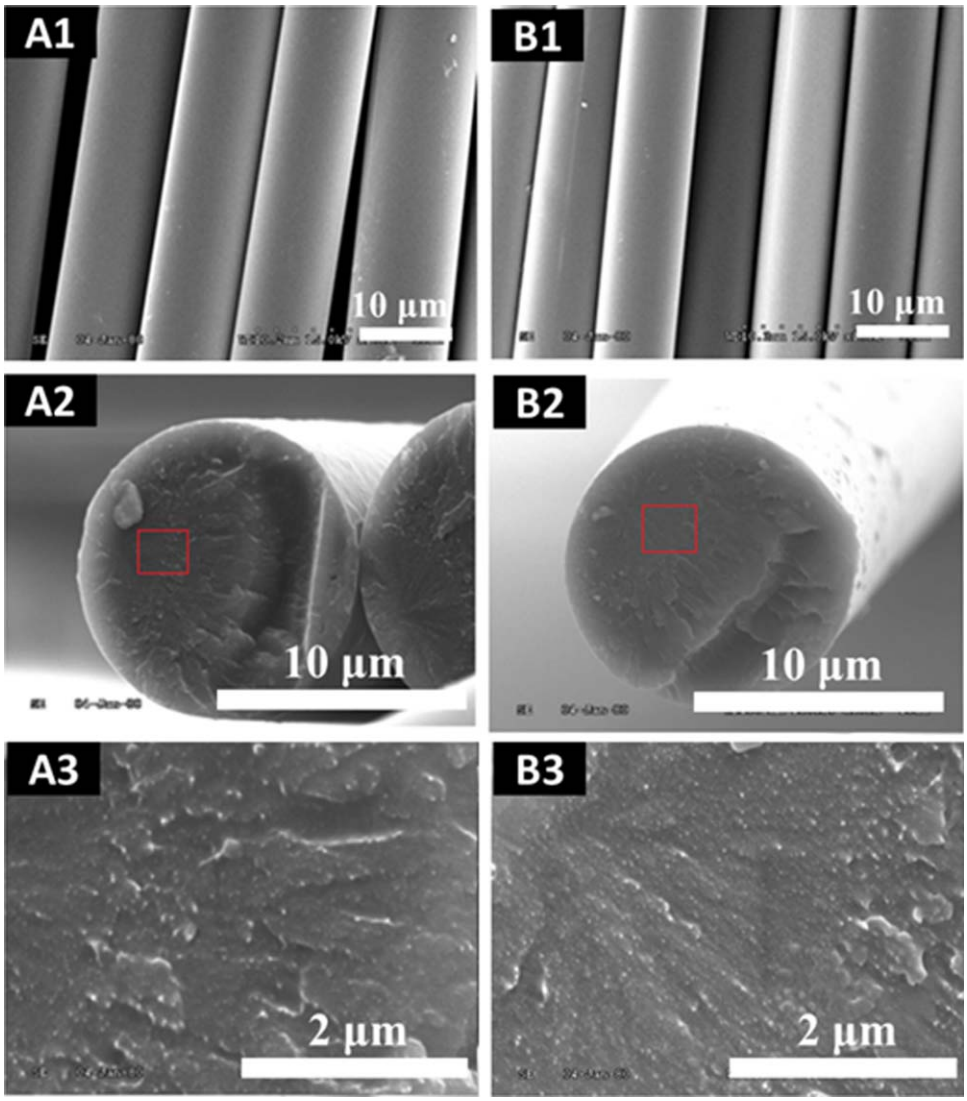

Figure 4. Scanning electron microscopy images of the surfaces and cross sections of as-spun PAA fibers with various dianhydride ratios: (A1–A3) PAA-0 and (B1–B3) PAA-3. [Color figure can be viewed in the online issue, which is available at wileyonlinelibrary.com.]

and facile method for setting up the temperature of the heating tube in the dry-spinning process in the preparation of precursor PAA fibers with higher initial IDs.

Morphology of the Dry-Spun PI Fibers

Figure 4 shows the scanning electron microscopy images of the surfaces and cross sections of the PAA-0 and PAA-3 as-spun fibers with various dianhydride ratios. These two precursor PAA fibers exhibited homogeneous surfaces and dense, uniform morphologies; these were beneficial for their good mechanical properties.

Aggregation Structure of the PI Fibers

As two of the basic structural parameters, the orientation and crystallinity of the fibers played important roles in the tensile properties of the polymeric fibers.[19,20] Figure 5 shows the WAXD patterns of the PI-1 and PI-3 fibers with various drawing ratios (λs). The as-spun fibers ($\lambda = 0$) both exhibited amorphous features. Dramatic changes occurred with increasing λs. For the PI-1 fiber, shown in Figure 5(A), the X-ray diffraction pattern revealed an oriented structure along the fiber axis (meridian direction) at $\lambda = 1.5$. Four brighter and narrower diffraction arcs were clearly observed when λ increased to 3.0; this revealed that a highly ordered structure along the meridian formed, and these four diffraction streaks were assigned to the (002), (004), (006), and (0010) planes. The scattering pattern along the meridian indicated a lamellar structure of the (00l) planes stacked parallel to the fiber axis. Meanwhile, with increasing λ, several diffraction arcs in the quadrants and clear diffraction points along the equator were observed; this indicated the formation of well-defined lateral packing order regions in the fibers. For details, one-dimensional WAXD intensity profiles along the equator and meridian for the PI-1 sample are shown in Figure 6(A,B). At high λs, several diffraction peaks corresponding to the (101/102/103), (010), and (110) planes along the equator gradually appeared. That is, a stretching-induced crystallization occurred in the heat drawing of the PI

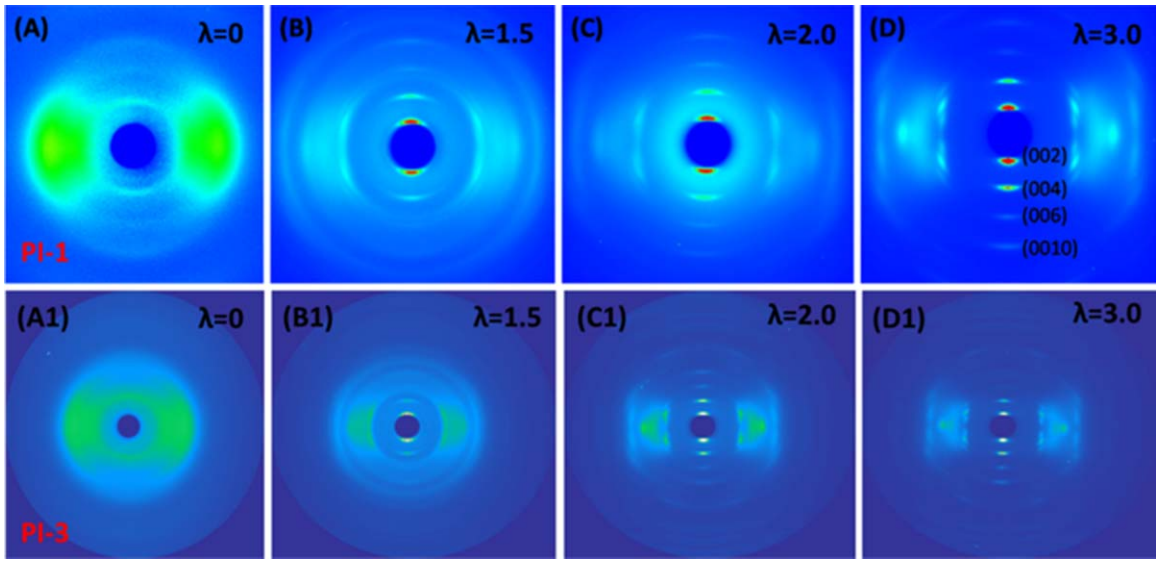

Figure 5. WAXD patterns of the (A–D) PI-1 fibers and (A1–D1) PI-3 fibers with various λs. [Color figure can be viewed in the online issue, which is available at wileyonlinelibrary.com.]

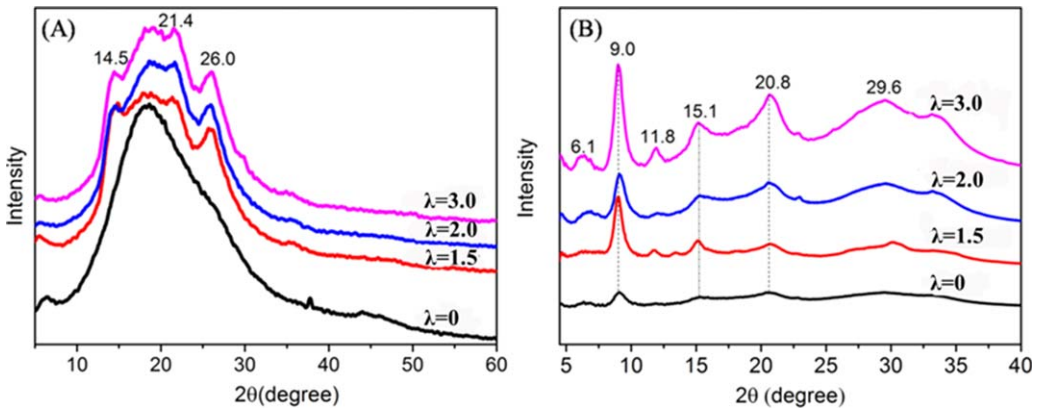

Figure 6. One-dimensional WAXD intensity profiles of PI-1 fibers with various λs: (A) equator and (B) meridian. [Color figure can be viewed in the online issue, which is available at wileyonlinelibrary.com.]

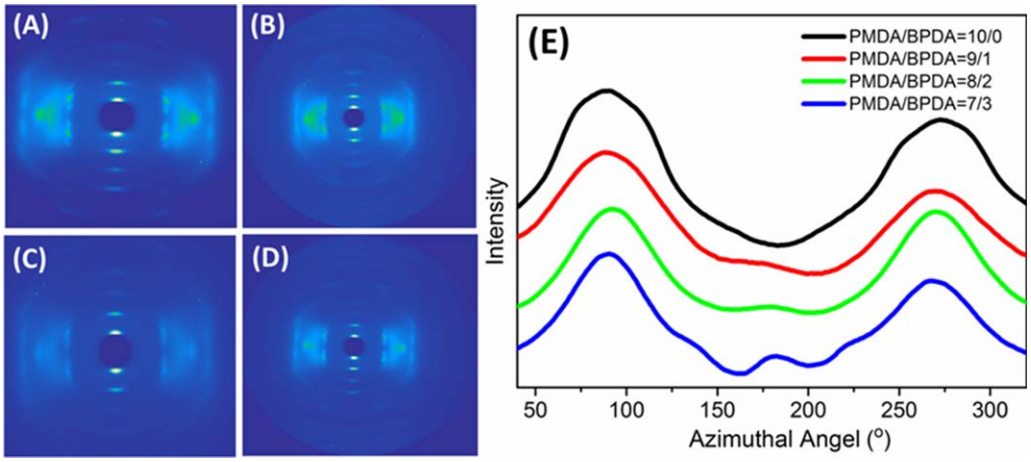

Figure 7. WAXD patterns of (A) PI-0, (B) PI-1, (C) PI-2, and (D) PI-3 and (E) azimuthal scan profiles of these four PI fibers with the same λ of 3.0. [Color figure can be viewed in the online issue, which is available at wileyonlinelibrary.com.]

Table I. Calculated f_cs of the Prepared PI Fibers

	f_c			
Sample	$\lambda = 0$	$\lambda = 1.5$	$\lambda = 2.0$	$\lambda = 3.0$
PI-0	0.38	0.60	0.77	0.92
PI-1	0.35	0.63	0.79	0.92
PI-2	0.37	0.67	0.81	0.94
PI-3	0.32	0.66	0.83	0.94

fibers. The PI-3 sample showed a much more diffuse reflection relatively; this indicated the gradual loss of the ordered packing regions. This resulted from the more or less random distribution of BPDA–ODA segments in the molecular chains. Additionally, the increased polymer chain mobility with greater BPDA contents was not beneficial for ordered chain packing compared with the rigid-rod PMDA/ODA.

The crystal orientation in the fibers was measured on the basis of the following Hermans' equation[21]:

$$f_c \times 100\% = [3 < \cos^2 \phi_c > -1]/2 \quad (2)$$

where f_c is the orientation factor along the fiber axis and ϕ_c is the angle between the fiber axis and the c axis. In our case, because the (002) crystallographic plane along the meridian is the most isolated, the numerical values for the mean-square cosine in eq. (2) were determined from the fully corrected intensity distribution diffracted from the (002) plane and intensity variation of the azimuthal angle of the (002) reflection [$I(\phi_c)$], averaged over the entire surface of the orientation sphere:

$$<\cos^2 \phi_c> = \frac{\int_0^{\frac{\pi}{2}} I(\phi_c)\cos^2 \phi_c \sin \phi_c d\phi_c}{\int_0^{\frac{\pi}{2}} I(\phi_c)\sin \phi_c d\phi_c} \quad (3)$$

where ϕ_c is the azimuthal angle of the (002) plane and d is the derivation. WAXD patterns and the azimuthal scan profiles from the (002) diffraction streak of these four PI fibers with the same λ (3.0) are shown in Figure 7. It was clear that these four samples all showed perfect crystalline and orientation structures. The calculated f_c values with various λs are listed in Table I. The degree of orientation increased with the continual stretching of the PI fibers; this was meaningful for the enhanced mechanical properties of these fibers.

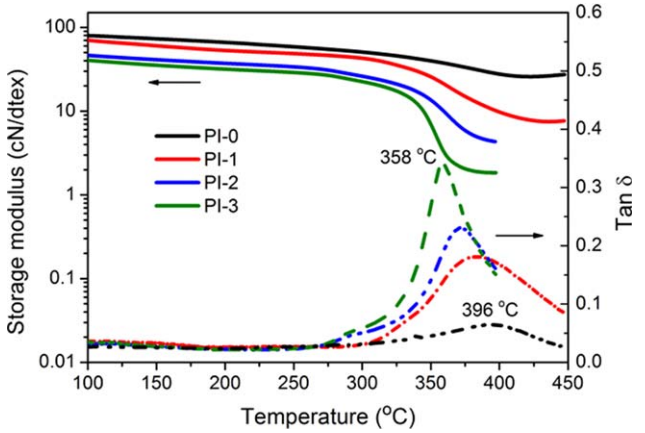

Figure 9. Dynamic E' and tan δ as a function of the temperature for the prepared PI fibers with various BPDA molar ratios. [Color figure can be viewed in the online issue, which is available at wileyonlinelibrary.com.]

Properties of the PI Fibers

The typical stress–strain diagram for these four PI fibers with the same λ (3.0) and detailed mechanical properties are shown in Figure 8. The PI-0 fiber possessed a tensile strength and modulus of 5.8 and 48.3 cN/dtex, respectively. When the molar ratio of the incorporated BPDA was over 20 mol %, the mechanical properties of the PI fibers were significantly enhanced, and the tensile strength and modulus for the PI-3 sample containing 30 mol % BPDA reached 8.55 and 73.21 cN/dtex. The significant improvement of the fibers' mechanical

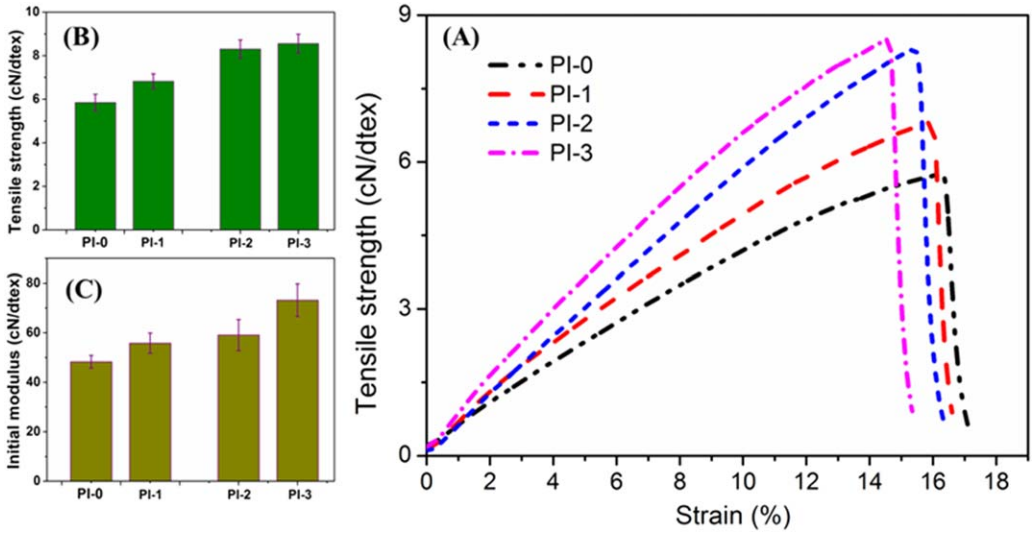

Figure 8. Mechanical properties of the dry-spun PI fibers with various dianhydride molar ratios and λ = 3.0: (A) stress–strain diagram; (B) tensile strength; and (C) modulus. [Color figure can be viewed in the online issue, which is available at wileyonlinelibrary.com.]

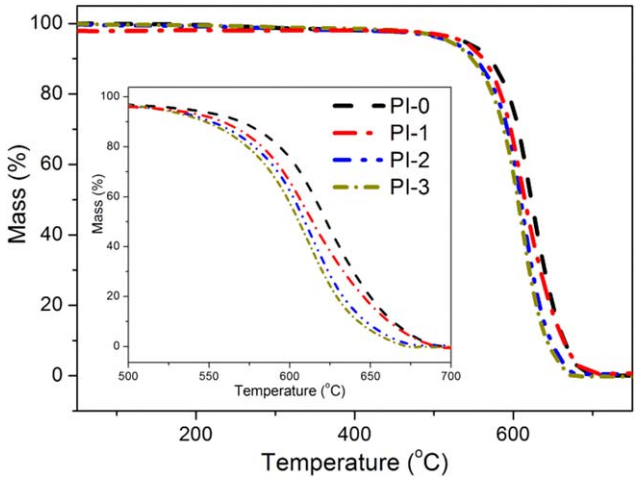

Figure 10. TGA curves of the PI fibers with various dianhydride molar ratios. [Color figure can be viewed in the online issue, which is available at wileyonlinelibrary.com.]

properties was mainly attributed to two factors: (1) increased macromolecule weights and (2) higher IDs.

Figure 9 shows the dynamic storage modulus (E') and tan δ as a function of the temperature for dry-spun PI fibers with various dianhydride molar ratios. The PI-0 fiber showed the highest E'; this was attributed to the rigid-rod chemical structure of PMDA–ODA. The introduction of BPDA into the polymer chains resulted in a decrease in E' because of the enhanced molecular mobility. An obvious relaxation process (α relaxation) was identified between 350 and 400 °C; this corresponded to the glass-transition temperature (T_g) of the PI segments. The detailed T_g values for PI-0 to PI-3 were 396, 384, 371, and 358 °C, respectively. Thus, the prepared PI fibers exhibited slightly lower T_g values with increasing BPDA content. Meanwhile, the intensities of the α relaxation gradually increased to a high level with the BPDA content. This variation of α relaxation represented the energy consumption in the polymer chain segmental motion. The previous WAXD results reflected the truth that the PI-0 fiber owned a more perfect crystalline structure and higher crystallinity; this resulted in restricted chain segmental motion and accounted for the higher T_g value and lower α relaxation intensities of the PI-0 fiber.

Table II. Thermal Properties and Dimensional Stability of the PI Fibers

Sample	T_g (°C)[a]	$T_{5\%}$ (°C)[b]	$T_{10\%}$ (°C)	Strain at 120 min (%)[c]
PI-0	396	546	571	−0.39
PI-1	384	541	563	−0.77
PI-2	371	537	553	−0.91
PI-3	358	525	547	−1.23
P84	—	—	—	−4.04

[a] Measured by DMA at 1 Hz and at a heating rate of 2 °C/min in nitrogen.
[b] Decomposition temperature recorded by TGA at a heating rate of 10 °C/min.
[c] Measured with a DMA instrument at 5 MPa and at a heating rate of 10 °C/min.

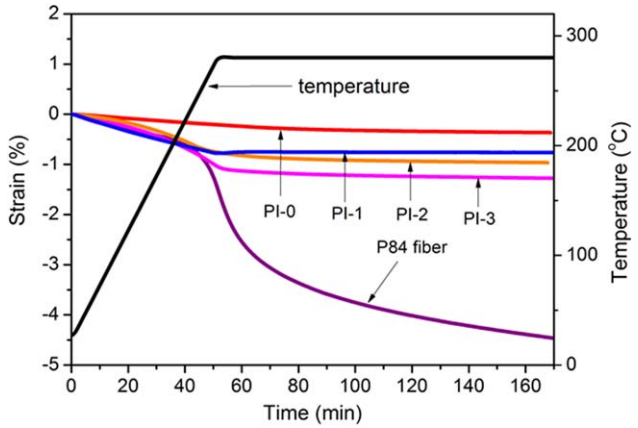

Figure 11. Changes in the strain for the PI fibers at a stress of 5 MPa. [Color figure can be viewed in the online issue, which is available at wileyonlinelibrary.com.]

TGA traces of the PI fibers under an air environment are shown in Figure 10, and the corresponding 5 and 10 wt % weight loss temperatures of the fibers in the TGA testing ($T_{5\%}$ and $T_{10\%}$, respectively) are listed in Table II. All of the samples showed similar pyrolysis behavior in air. The $T_{5\%}$ values for PI-0 to PI-3 ranged from 546 to 525 °C; this demonstrated the excellent thermooxidative stabilities of the prepared PI fibers. The samples containing BPDA units show slightly decreased $T_{5\%}$ and $T_{10\%}$ values; this indicated that the introduction of the biphenyl moiety had a small negative effect on the thermal stability of the PI fibers.

The thermal dimensional stability was of importance for the high-performance polymeric fibers. Figure 11 shows the changes in the strain versus time during the fibers' heating treatment. For comparison, the commercialized P84 fiber with a chemical structure of BTDA/MDI/TDI was also tested under the same conditions. All of the samples exhibited negative strain values when they were heated at a stress of 5 MPa; this indicated the shrinkage behavior of these fibers. Obviously, the P84 fiber showed an abruptly quick shrinkage around 246 °C, whereas the dry-spun PI fibers changed slightly. The corresponding strain values at 120 min of these fibers are listed Table II. The P84 fiber owned a strain value of −4.01%; this was 2.3 times larger than the PI-3 fiber. This indicated better dimensional stability of the prepared PI fibers.

CONCLUSIONS

PI fibers containing biphenyl units were successfully prepared by a typical two-step dry-spinning process based on three monomers, PMDA, ODA, and BPDA. The incorporated BPDA units apparently enhanced the molecular mobility of the polymer chains. This showed positive effects on the thermal imidization of the precursor fibers. The WAXD results indicate that these resulting PI fibers had a three-dimensional ordered arrangement of the molecular chains. These factors indicated that the optimum mechanical properties of the prepared fibers with a tensile strength and modulus of 8.55 and 73.21 cN/dtex, respectively, when the molar ratio of PMDA/BPDA was 7/3. Moreover, the T_g values of these samples ranges from 396 to 358 °C, and $T_{5\%}$ in air was 546–525 °C; this showed their excellent thermal stability.

ACKNOWLEDGMENTS

This work was financially supported by the National Science Foundation of China (contract grant numbers 51233001 and 51173024) and the 973 Plan (contract grant number 2014CB643603). WAXD experiments were performed at the 16B1 Beamline Station of the Shanghai Synchrotron Radiation Facility.

REFERENCES

1. Yin, C.; Dong, J.; Zhang, D.; Lin, J.; Zhang, Q. H. *Eur. Polym. J.* **2015**, *67*, 88.
2. Niu, H.; Huang, M.; Qi, S.; Han, E.; Tian, G.; Wang, X.; Wu, D. Z. *Polymer* **2013**, *54*, 1700.
3. Liu, X.; Gao, G.; Dong, L.; Ye, G.; Gu, Y. *Polym. Adv. Technol.* **2009**, *20*, 362.
4. Zhao, Y.; Hu, S.; Liu, W.; An, G.; Wu, Z.; Wu, D.; Jin, R. *High Perform. Polym.* **2015**, *27*, 153.
5. Kim, Y. J.; Lee, S. M.; Kim, S. H.; Kim, H. S. J. *Electrochem. Sci. Technol.* **2015**, *6*, 26.
6. Zheng, F.; Zhang, X.; Zhao, G.; Wang, Q.; Wang, T. *J. Appl. Polym. Sci.* **2014**, 131, DOI: 10.1002/app.40774.
7. Chen, B.; Yang, J.; Wang, J.; Liu, N.; Li, H.; Yan, F. *Polym. Compos.* **2014**, DOI: 10.1002/pc.23337.
8. Xiang, H. B.; Huang, Z.; Liu, L. Q.; Chen, L.; Zhu, J.; Hu, Z. M.; Yu, J. R. *Macromol. Res.* **2011**, *19*, 645.
9. Guo, B.; Zhang, Y.; Chen, L.; Yu, J.; Zhu, J.; Hu, Z. *High Perform. Polym.* **2014**.
10. Kakvan, A.; Shaikhzadeh Najar, S.; Psikuta, A. *J. Text. Inst.* **2015**, *106*, 674.
11. Lua, A. C.; Su, J. *Polym. Degrad. Stab.* **2006**, *91*, 144.
12. Xu, Y.; Wang, S.; Li, Z.; Xu, Q.; Zhang, Q. *J. Mater. Sci.* **2013**, *48*, 7863.
13. Dong, J.; Xu, Y.; Xia, Q.; Yin, C.; Zhang, Q. H. *High Perform. Polym.* **2014**, *26*, 517.
14. Wang, Y.; Yang, Y.; Jia, Z.; Qin, J.; Gu, Y. *J. Appl. Polym. Sci.* **2013**, *127*, 4581.
15. Pramoda, K. P.; Liu, S.; Chung, T. S. *Macromol. Mater. Eng.* **2002**, *287*, 931.
16. Kotera, M.; Nishino, T.; Nakamae, K. *Polymer* **2000**, *41*, 3615.
17. Dimitrakopoulos, C. D.; Machlin, E. S.; Kowalczyk, S. P. *Macromolecules* **1996**, *29*, 5818.
18. Kreuz, J. A.; Endrey, A. L.; Gay, F. P.; Sroog, C. E. *J. Polym. Sci. Part A-1: Polym. Chem.* **1966**, *4*, 2607.
19. Eashoo, M.; Wu, Z.; Zhang, A.; Shen, D.; Tse, C.; Harris, F. W.; Cheng, S. Z.; Gardner, K. H.; Hsiao, B. S. *Macromol. Chem. Phys.* **1994**, *195*, 2207.
20. Dong, J.; Yin, C.; Lin, J.; Zhang, D.; Zhang, Q. *RSC Adv.* **2014**, *4*, 44666.
21. Zhang, M.; Niu, H.; Lin, Z.; Qi, S.; Chang, J.; Ge, Q.; Wu, D. *Macromol. Mater. Eng.* **2015**, *300*, 1096.

SGML and CITI Use Only
DO NOT PRINT